



# Proposal of a new diffractive corneal inlay to improve near vision in a presbyopic eye

DIEGO MONTAGUD-MARTÍNEZ,<sup>1</sup> VICENTE FERRANDO,<sup>1</sup> JUAN A. MONSORIU,<sup>1</sup>  AND WALTER D. FURLAN<sup>2,\*</sup> 

<sup>1</sup>Centro de Tecnologías Físicas, Universitat Politècnica de València, Valencia 46022, Spain

<sup>2</sup>Departamento de Óptica y Optometría y Ciencias de la Visión, Universitat de València, Burjassot 46100, Spain

\*Corresponding author: walter.furlan@uv.es

Received 19 November 2019; revised 21 January 2020; accepted 22 January 2020; posted 23 January 2020 (Doc. ID 383581); published 27 February 2020

**A new class of diffraction-based corneal inlays for treatment of presbyopia is described. The inlay is intended to achieve an improvement of the near focus quality over previous designs. Our proposal is a two-zone hybrid device with separated amplitude and phase areas having a central aperture and no refractive power. An array of micro-holes is distributed on the surface of the inlay conforming a binary photon sieve. In this way, the central hole of the disk contributes to the zero order of diffraction, and the light diffracted by the micro-holes in the peripheral photon sieve produces a real focus for near vision. We employed ray-tracing software to study the performance of the new inlay in the Liou–Brennan model eye. The modulation transfer functions (MTFs) at the distance and near foci, and the area under the MTFs for different object vergences, were the merit functions used in the evaluation. The results were compared with those obtained with previous pure amplitude designs. Additionally, image simulations were performed with the inlays in the model eye to show the good performance of our proposal in improving the quality of the near vision.** © 2020 Optical Society of America

<https://doi.org/10.1364/AO.383581>

## 1. INTRODUCTION

Corneal inlays are optical devices employed by ophthalmologists to provide good near and intermediate vision of presbyopic people between the ages of 45 and 60 years old. As their name suggests, corneal inlays are surgically implanted within the corneal stroma (the thicker middle layer of the cornea) into a small pocket created with a femtosecond laser. The pocket seals itself, and the entire procedure typically takes only a few minutes. Actually, corneal inlay surgery is less invasive than other procedures, which involve implanting intraocular lenses inside the eye, either directly in front of or behind the iris. Moreover, corneal inlay surgery is usually combined with LASIK surgery to correct both presbyopia and refractive defects [1–3].

Considering their physical operating principles, corneal inlays can be classified into different categories: refractive inlays, small aperture inlays, and diffractive inlays [2,4], with the last category being the most recent development in this field. In fact, in Ref. [4] our team reported the first amplitude diffractive corneal inlay (ADCI) as the result of the combination of two concepts: the pin-hole effect [5] (used in the above-mentioned small aperture inlays) and the photon sieve [6,7] (a photon sieve is essentially an amplitude Fresnel zone plate in which the transparent rings have been replaced by a set of non-overlapping holes distributed within the corresponding area).

Recently we have studied different designs of ADCI in comparison with small aperture corneal inlay, both numerically in different model eyes [8,9] and also experimentally *in vitro* with ADCI prototypes [9]. Those studies revealed that ADCI exhibits a higher light throughput, and improvements in imaging of near objects. In an effort to further improve the near vision of presbyopic people, here we present a new class of diffraction-based corneal inlays. The fundamental difference with the previous ADCI models is that it is a hybrid device with two concentric ring areas: the inner one having a pure phase transmittance and the outer one having a pure amplitude transmittance. Thus, the new model, called hybrid diffractive corneal inlay (HDCI), is a solid ring in which these two differentiated parts are drilled with an array of micro-holes distributed on the surface of the inlay conforming a binary photon sieve. In this way, the central hole of the disk contributes to the zero order of diffraction, and the light diffracted by the micro-holes in the peripheral photon sieve produces a real focus for near vision. We employed Zemax OpticStudio software to study the performance of the new inlay in the Liou–Brennan model eye. The merit functions we used in the evaluation of the HDCI were the modulation transfer function (MTF) at the distance and near foci, and the area under the MTFs (AMTFs) for different object vergences. Results were compared with those obtained with

an equivalent ADCI. Additionally, the point spread functions (PSFs) were computed and image simulations were performed with the inlays in the model eye to evaluate the performance of our proposal.

### 2. DIFFRACTIVE CORNEAL INLAYS

To describe the HDCI design, let us recall that previous designs of ADCI were considered [8] in which both the radius of the central hole and the area covered by the surrounding photon sieve structure were varied to obtain different ratios of energy between the near and far foci. The higher values of the axial irradiance at the near focus were obtained with the design shown in Fig. 1(a), where the black region represents the opaque surface (with zero transmittance), while the white regions are holes drilled on the opaque surface, so these are transparent regions with transmittance value 1 and phase 0. To improve the efficiency of the near focus we have considered a hybrid design in which the innermost three opaque rings were replaced with transparent rings of thickness  $h$  equivalent to a phase change of  $\pi$ . So,

$$h = \frac{\lambda_0}{2 \cdot (n_{CI} - n_c)}, \tag{1}$$

where  $\lambda_0$  is the design wavelength,  $n_{CI}$  is the refractive index of the corneal inlay material, and  $n_c$  is the refractive index of the cornea. In this way, a half-wave phase shift is provided between the holes and the transparent region at the central part of the inlay. The HDCI transmittance distribution is shown in Fig. 1(b), where the transparent surface with  $\pi$  phase is represented in blue. As can be seen in this figure, the HDCI evaluated in this study consisted of a disk of 4.15 mm diameter with a central hole of 1.00 mm diameter surrounded by the three innermost transparent rings up to a radius of 1.133 mm and other seven outermost opaque rings up to the external radius of the inlay. In this way, the effect of the combination of phase and amplitude in the HDCI can be appreciated, even for the smallest pupil we considered in this work [see the green circle in Fig. 1(b)]. Both ADCI and the HDCI have a total of 9640 holes of different sizes, the smallest ones being 18  $\mu\text{m}$  in diameter. They were designed to provide a near diffractive focus

corresponding to a nominal addition of +3.00 D for the design wavelength (550 nm).

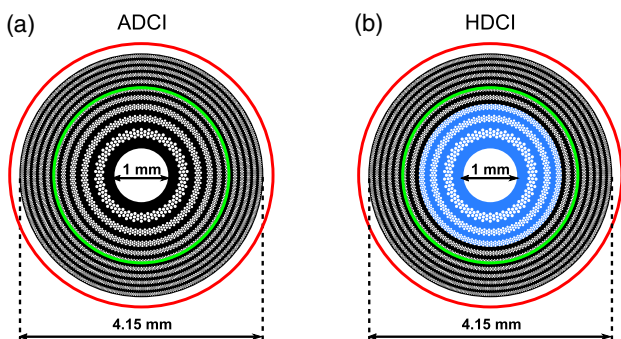
By using Eq. (1) we have found that the structure of the inlay must have a thickness of  $h = 4.91 \mu\text{m}$ . The same thickness was considered for the ADCI in the following analysis.

### 3. RESULTS

To validate the HDCI design the Zemax OpticStudio optical design software (<http://www.zemax.com/os/opticstudio>) was employed to simulate the theoretical model eye proposed by Liou and Brennan [10]. This model eye is especially well adapted to investigate the optical properties of corneal inlays because it was designed using biometric data obtained from patients aged around 45 years (early presbyopes). Additionally, the Liou–Brennan model eye has an aspheric cornea, a decentered pupil (0.5 mm in the nasal direction), a lens with refractive index gradients in the axial and radial directions, and a visual axis tilted 5° to the optical axis (kappa angle). The ADCI and the HDCI were sequentially positioned in this model eye at a depth of 0.20 mm from the anterior corneal surface according to the surgical procedure followed for other types of amplitude corneal inlays like Kamra [3]. Within this model the entrance and exit pupils were located at 3.1 mm and -at -26.3 in front of the cornea and the retina, respectively. Table 1 shows the data sheet used in the simulations. The ADCI was introduced as a *User Defined Aperture* (.uda file), since with this kind of file the locations of the holes in the inlay surface and their dimensions can be easily programmed. On the other hand, the HDCI was simulated by a *Grid Sag Surface* with the phase corresponding to the inner three rings superimposed to another .uda file similar to the one employed for the ADCI but with an internal radius of 1.133 mm (see Fig. 1). Two different pupil diameters were evaluated: 3.0 mm and 4.5 mm, simulating photopic and mesopic conditions. Monochromatic light of 550 nm was considered in the analysis, coincident with the design wavelength of the inlays, which corresponds to the maximum sensitivity of the human eye in photopic conditions [11].

To evaluate the optical quality of the inlays shown in Fig. 1, the MTFs were measured for objects at different vergences, in 0.1 D steps between +0.50 D and -3.50 D. Since the theoretical model eye is asymmetric, the ray-tracing program calculates the sagittal and tangential MTFs and, therefore for each vergence, both MTFs were averaged to obtain the MTFs shown in the following results. Figure 2 shows MTFs at far and near foci for both corneal inlays with both pupillary conditions. Note that the MTFs for near vision are shown in logarithmic scale in order to better appreciate the differences between both designs. As can be noted in near vision for both pupils, the MTFs provided by the HDCI are better since the phase structure at the transparent area of the HDCI improves the diffraction efficiency, increasing the amount of light directed to the near focus. On the other hand, for distant vision the ADCI provides the best MTFs.

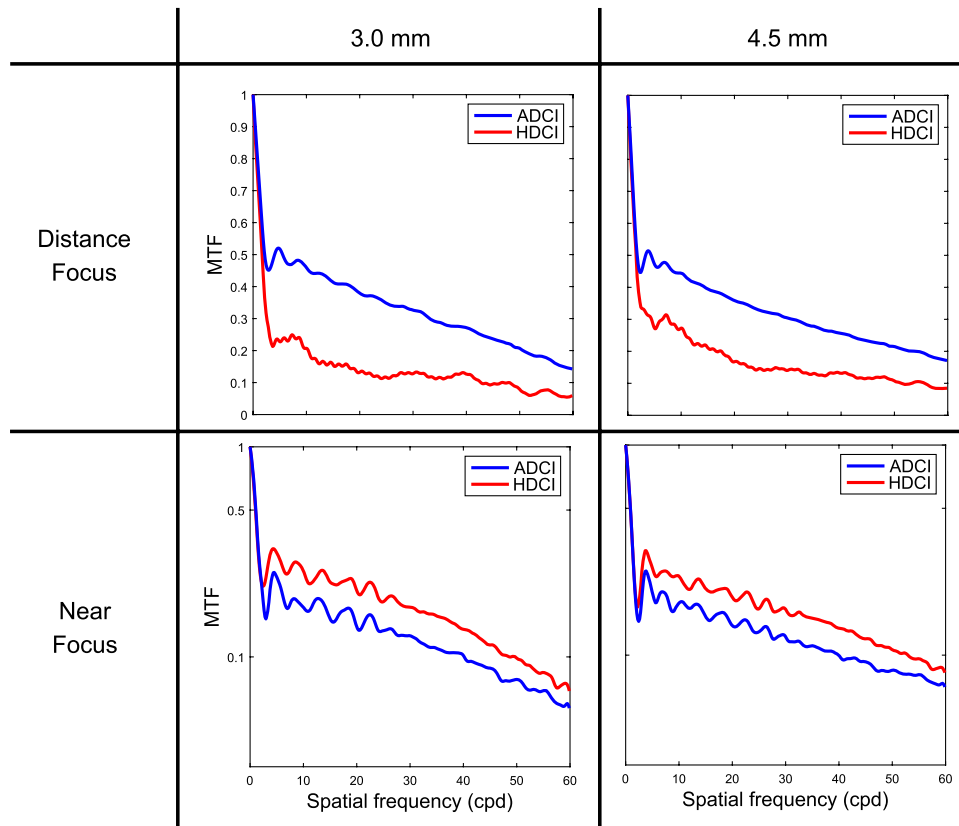
To give insight into how the relative image quality for distance and near objects is provided by both designs, the AMTF has been calculated. In fact, this metric showed a high correlation with the visual acuity [12]. In our case we have selected the range of spatial frequencies between 9.5 cycles per degree and



**Fig. 1.** Structure of the corneal inlays evaluated in this study. The black regions are opaque. While the white and blue zones are transparent with a phase 0 and  $\pi$  phase, respectively. The green and red circles represent the pupil diameters considered in the numerical assessment of the inlays: 3.0 mm and 4.5 mm, respectively.

**Table 1.** Liou–Brennan Model Eye Zemax Data Sheet ( $r$  and  $z$  are Radial and Axial Coordinates in the Crystalline Lens)

Surface	Radius (mm)	Asphericity	Thickness (mm)	Refractive Index
Anterior Cornea	7.77	-0.18	0.200	1.376
Anterior corneal inlay	7.77	-0.18	0.005	1.376 (ADCI) 1.432 (HDCI)
Posterior corneal inlay	7.77	-0.18	0.295	1.376
Posterior Cornea	6.40	-0.60	3.160	1.336
Iris	—	—	0.000	—
Anterior Lens	12.40	-0.94	1.590	$1.368 + 0.049057 z - 0.015427 z^2 - 0.001978 r^2$
Lens	Infinity	—	2.430	$1.407 - 0.006605 z^2 - 0.001978 r^2$
Posterior Lens	-8.10	0.96	16.260	1.336

**Fig. 2.** MTFs for distance and near foci provided by the ADCI (blue) and by the HDCI (red) with pupil diameters of 3.0 mm and 4.5 mm.

30 cycles per degree, equivalent to visual acuities between 0.5 logMAR and 0.0 logMAR. Figure 3 shows the AMTFs provided by the corneal inlays with different pupils. As can be seen, both designs have a bifocal profile but for both pupil diameters, the near focus the HDCI presents a higher value of the AMTF with an extended depth of focus, in comparison with the ADCI. On the other hand, as expected from the results shown in Fig. 2, the ADCI has a better performance for distance objects.

To complete our analysis, the PSFs provided for the HDCI and the ADCI were also obtained at distance and near foci for both models. Additionally, simulated images of a tumbling  $E_s$  optotype were obtained for two pupil diameters. The results are shown in Figs. 4 and 5. The optotype with letter sizes corresponding to visual acuities 0.4, 0.2, and 0 in the logMAR scale has been convolved with the PSFs in order to obtain the image simulation using a custom MATLAB code (Mathworks,

Inc. R2018b). The PSFs provided by Zemax are shown in these figures and were normalized by the software to their respective maximum values. However, the PSF used in the convolution with the object were rescaled and normalized with respect to their total energy of the PSF to obtain images in which the contrast can be directly compared. These results also confirm the results obtained in Figs. 2 and 3; i.e., the images of near objects with the HDCI are better than those obtained with ADCI for both pupil diameters. In fact, in both cases the Weber contrast, defined as  $C = (L_{\max} - L_{\min}) / L_{\text{Background}}$ , where  $L_{\max}$ ,  $L_{\min}$ , and  $L_{\text{Background}}$  are luminance maximum, minimum, and background, respectively, improved by 3.5%. Finally, to show the extended depth of focus for near vision, images simulations were obtained at object vergence of 2.5 D. The results are shown in Fig. 6. The better performance at near of the HDCI can be clearly seen in this figure.

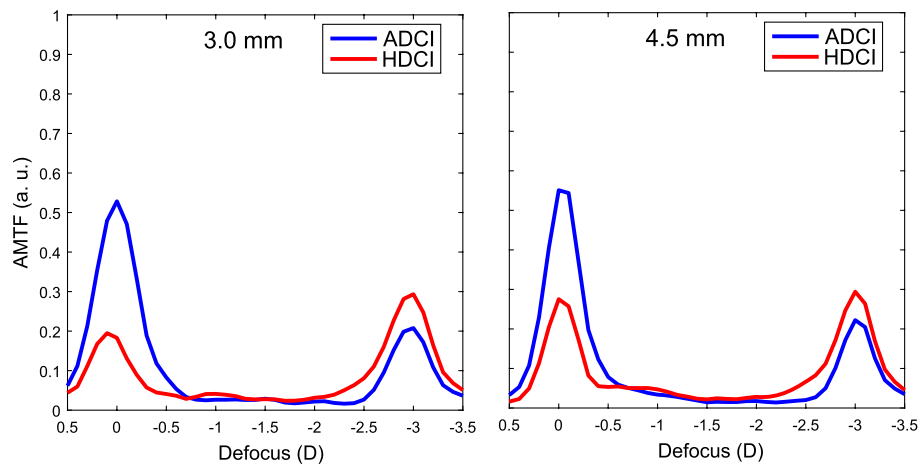


**Fig. 3.** Through the focus AMTFs for both inlays: ADCI (blue) and HDCI (red).

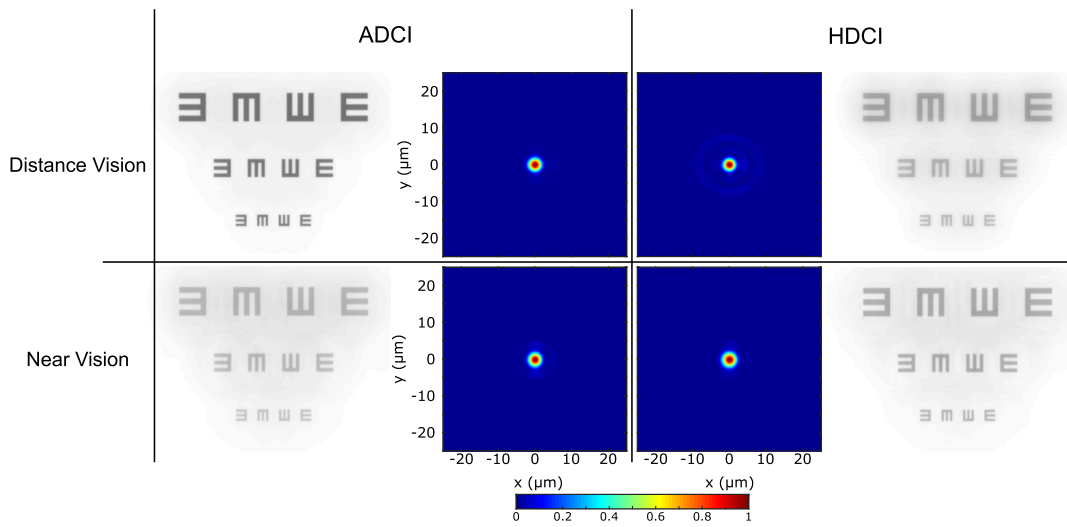


**Fig. 4.** PSFs and image simulation of both corneal inlays in distance and near vision for 3.0 mm of pupil.

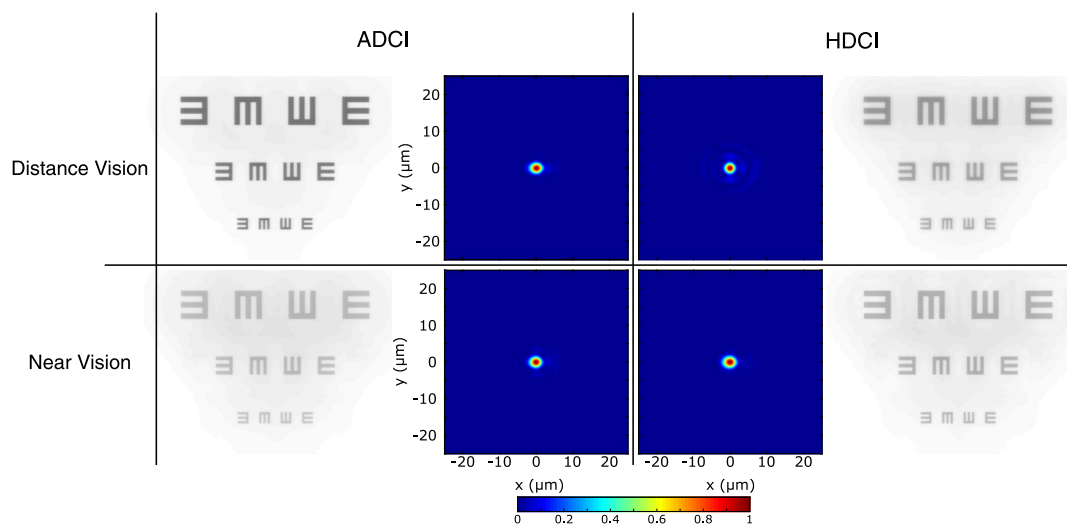


**Fig. 5.** PSFs and image simulation of both corneal inlays in distance and near vision for 4.5 mm of pupil.

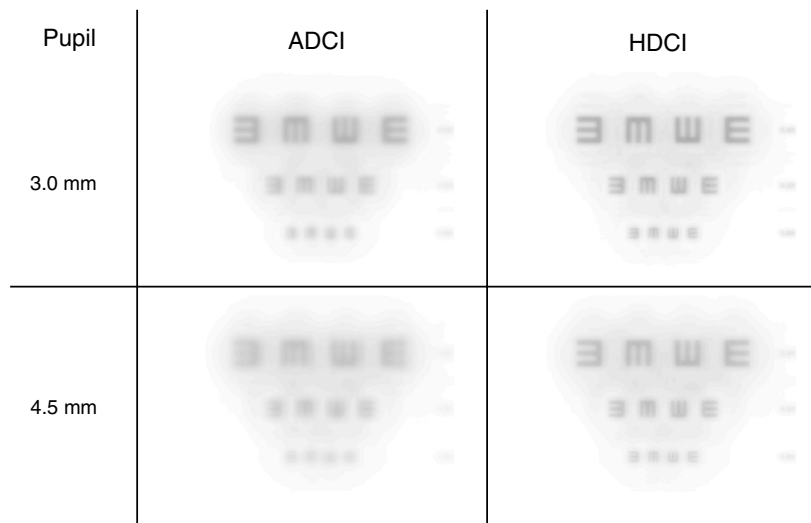


**Fig. 6.** Image simulation of both corneal inlays at object vergence of 2.5 D, which corresponds to a defocus of 0.5 D relative to the near focus shown in Figs. 4 and 5.

#### 4. CONCLUSIONS

Diffractional corneal inlays are the newest type of corneal implants designed for the treatment of presbyopia. Previous designs consisted of pure amplitude models having different construction parameters (such as the central hole radius, the inlay diameter, addition, number and distribution of micro-holes) that provide different results, proving that diffractive corneal inlays could be customized to meet different patients' needs [8,9]. In this work we added a new variable to the design parameters of diffractive corneal inlays, which consists of introducing a transparent region on the diffractive surface to improve the diffraction efficiency of the near focus. The performance of the resulting model, HDCI, was compared with an equivalent amplitude model, ADCI, with the same number and distribution of micro-holes. With the new model we found an improvement of the near focus efficiency, and an extension of the depth of focus for near. However, these benefits were obtained at the cost of losing contrast for distance objects, and it seems that the previous design provides an overall better optical quality. Now, taking into account that normally corneal inlays are implanted monocularly in the non-dominant eye [3], this fact is not necessarily a great disadvantage for distance vision, because the fellow eye could compensate for this.

Thus, in further studies the HDCI will be analyzed under different realistic variations that affect its optical properties, such as the influence of the inlay decentration and its behavior under polychromatic illumination. Moreover, both designs need to be tested subjectively to assess their performance.

**Funding.** Ministerio de Economía y Competitividad, Spain (2019/048, DPI 2015-71256-R); Conselleria d'Educació, Investigació, Cultura i Esport, Comunitat Valenciana, Spain (PROMETEO/2019/048).

**Acknowledgment.** Portions of this work were presented at the Optics Meeting (RIO), the Latin American Meeting in Optics, Lasers and Applications (OPTILAS), and the Mexican

Optics and Photonics Meeting (MOPM) in September 2019, "Diffractional corneal inlays: ray tracing analysis in a model eye."

D. Montagud-Martínez and V. Ferrando acknowledge the financial support from the Universitat Politècnica de València, Spain (fellowships FPI-2016 and PAID-10-18, respectively).

**Disclosures.** The authors declare no conflicts of interest.

#### REFERENCES

1. R. L. Lindstrom, S. M. Macrae, J. S. Pepose, and P. C. Hoopes, "Corneal inlays for presbyopia correction," *Curr. Opin. Ophthalmol.* **24**, 281–287 (2013).
2. W. N. Charman, "Developments in the correction of presbyopia II: surgical approaches," *Ophthalmic Physiol. Opt.* **34**, 397–426 (2014).
3. E. M. Art, E. M. Krall, S. Moussa, G. Grabner, and A. K. Dextl, "Implantable inlay devices for presbyopia: the evidence to date," *Clin Ophthalmol.* **9**, 129–137 (2015).
4. W. D. Furlan, S. García-Delpech, P. Udaondo, L. Remón, V. Ferrando, and J. A. Monsoriu, "Diffractional corneal inlay for presbyopia," *J. Biophotonics* **10**, 1110–1114 (2017).
5. C. Trindade, "Small aperture (pinhole) intraocular implant to increase depth of focus," U.S. Patent Application No. 14/297,447 (5 June 2014).
6. L. Kipp, M. Skibowski, R. L. Johnson, R. Berndt, R. Adelung, S. Harm, and R. Seemann, "Sharper images by focusing soft X-rays with photon sieves," *Nature* **414**, 184–188 (2001).
7. F. Giménez, J. A. Monsoriu, W. D. Furlan, and A. Pons, "Fractal photon sieve," *Opt. Express* **14**, 11958–11963 (2006).
8. D. Montagud-Martínez, V. Ferrando, F. Machado, J. A. Monsoriu, and W. D. Furlan, "Imaging performance of a diffractive corneal inlay for presbyopia in a model eye," *IEEE Access* **7**, 163933 (2019).
9. D. Montagud-Martínez, V. Ferrando, J. A. Monsoriu, and W. D. Furlan, "Optical evaluation of new designs of multifocal diffractive corneal inlays," *J. Ophthalmol.* **2019**, 9382467 (2019).
10. H. L. Liou and N. A. Brennan, "Anatomically accurate, finite model eye for optical modeling," *J. Opt. Soc. Am. A* **14**, 1684–1695 (1997).
11. H. Gross, F. Blechinger, and B. Achnert, *Handbook of Optical Systems* (Wiley, 2008), Vol. 4, Survey of Optical Instruments.
12. A. Alarcon, C. Canovas, R. Rosen, H. Weeber, L. Tsai, K. Hileman, and P. Piers, "Preclinical metrics to predict through-focus visual acuity for pseudophakic patients," *Biomed. Opt. Express* **7**, 1877–1888 (2016).